Molecular View of Hexagonal Phase Formation in Phospholipid Membranes

Siewert-Jan Marrink and Alan E. Mark
Department of Biophysical Chemistry, University of Groningen, 9747 AG Groningen, The Netherlands

ABSTRACT Important biological processes, such as vesicle fusion or budding, require the cell matrix to undergo a transition from a lamellar to a nonlamellar state. Although equilibrium properties of membranes are amenable to detailed theoretical studies, collective rearrangements involved in phase transitions have thus far only been modeled on a qualitative level. Here, for the first time, the complete transition pathway from a multilamellar to an inverted hexagonal phase is elucidated at near-atomic detail using a recently developed coarse-grained molecular dynamics simulation model. Insight is provided into experimentally inaccessible data such as the molecular structure of the intermediates and the kinetics involved. Starting from multilamellar configurations, the spontaneous formation of stalks between the bilayers is observed on a nanosecond timescale at elevated temperatures or reduced hydration levels. The stalks subsequently elongate in a cooperative manner leading to the formation of an inverted hexagonal phase. The rate of stalk elongation is $\sim$0.1 nm ns^{-1}. Within a narrow hydration/temperature/composition range the stalks appear stable and rearrange into the rhombohedral phase.

INTRODUCTION

Phospholipids, one of the main components of cell membranes may adopt a variety of phases. Depending on the balance between attractive forces in the headgroup region and repulsive forces between the lipid tails, phases with a positive curvature (e.g., micellar), no curvature (lamellar), or a negative curvature (e.g., inverted hexagonal) are preferred. Transitions between these phases can be triggered by altering the balance of forces, for instance by changes in temperature or hydration. The transition from a lamellar to an inverted hexagonal phase is of particular importance, especially in biological systems. This is because the intermediates in this process are believed to involve the formation of interlamellar stalks (Siegel and Epand, 1997; Siegel, 1999). Within cells stalk formation is also believed to be the first step in membrane fusion (Kozlov and Markin, 1983; Chernomordik et al., 1987; Marrink and Mark, 2003). Evidence for a stalk intermediate in lamellar to hexagonal phase transitions has come recently from the discovery of a stable phospholipid stalk phase, the rhombohedral phase (Yang and Huang, 2002).

In this phase, which is in between the lamellar and the inverted hexagonal phase, stalks are ordered in a hexagonal pattern. For DOPC/DOPE mixtures the effective spontaneous curvature can be tuned by changes in composition. As a consequence, the phase diagram of DOPC/DOPE mixtures has regions where either a lamellar or an inverted hexagonal phase can occur, and a narrow range in which the rhombohedral phase is observed (Yang et al., 2003). The DOPC/DOPE mixture therefore provides an ideal model system for studying phase transitions. Here we apply molecular dynamics (MD) simulations to elucidate the molecular details of the phase transitions of DOPC/DOPE mixtures. The simulations are based on a recently developed coarse-grained (CG) lipid model (Marrink et al., 2004). The model reproduces many of the structural, dynamic, and elastic properties of both lamellar and nonlamellar states of a variety of phospholipids. The ability to reproduce phase diagrams of lipid systems on a quantitative level opens the way to explore the complex behavior of realistic processes involving cell membranes in near-atomic detail.

METHODS

CG model

In the CG model, which is based on the pioneering work of Smit et al. (1990), small groups of atoms (4–6 heavy atoms) are united into single interaction centers. All particles interact through pairwise short-range Lennard-Jones (LJ) potentials. The strength of the interaction depends on the nature of the particles. The particles differ in their degree of hydrophilicity. Hydrophilic particles are attracted more strongly to other hydrophilic particles than to hydrophobic particles. The inset in Fig. 2 shows the CG representation of DOPE, consisting of twelve interaction sites. The lipid headgroup consists of two hydrophilic particles, one representing the choline (PC) or ethanolamine (PE) site and one representing the phosphate group. With respect to the choline particle the interaction of the ethanolamine particle to other ethanolamine particles or to the glycerol particles is stronger, mimicking the enhanced hydrogen-bonding capability of the PE group. Two sites of intermediate hydrophilicity are used to represent the glycerol moiety. Each of the two tails is modeled by five hydrophobic sites. The solvent is modeled by hydrophilic particles each representing four ''real'' water molecules. In addition to the LJ interactions, a screened Coulombic interaction is used to model the electrostatic interaction between the zwitterionic headgroups. Bonded interactions are modeled by a weak harmonic potential. Angle potentials provide the appropriate stiffness for the lipid molecule, and model the unsaturation of the oleoyl tails. The effective timescale for this CG model was determined by relating the diffusion rate of the solvent to the experimental self-diffusion rate of bulk water and validated by examining other experimentally accessible dynamical properties, such as

Submitted June 30, 2004, and accepted for publication September 2, 2004.

Address reprint requests to Siewert-Jan Marrink, Tel.: 31-50-363-4339; Fax: 31-50-363-4800; E-mail: marrink@chem.rug.nl.

0006-3495/04/12/3894/07 $2.00

doi: 10.1529/biophysj.104.048710

the lipid lateral diffusion rates in bilayers and the permeation rate of water across a bilayer, all of which were reproduced. A full description of the model can be found in Marrink et al. (2004). There was one difference between the model used in this article and the one published in Marrink et al. (2004). The phosphate-water LJ interaction was increased from 5.0 to 5.8 kJ/mol. This increases the hydration level of the bilayer slightly, improving the line tension of phospholipid bilayers. The lamellar-to-inverted hexagonal phase transition using the previously published model proceeds via the same mechanism as is presented in this article. However, the hexagonal phase is stabilized in comparison to the version used for the current simulations.

State conditions simulated

A schematic composition/temperature/hydration phase diagram for DOPC/DOPE is shown in Fig. 1. The diagram is based on experimental measurements of pure DOPE by Rand and Fuller (1994) and mixed DOPC/DOPE by Yang and Huang (Yang et al., 2003). In the experiments of Rand and Fuller the amount of water per lipid is controlled by adding a specific amount of water to dry lipid (gravimetric samples). Yang and Huang performed humidity controlled measurements. With this method the chemical potential of water within the sample is fixed. The hydration level can thus be carefully controlled, but the absolute number of waters/lipid can not be determined directly. In the phase diagram it is assumed that the hydration range for the mixed systems is similar to that observed for pure DOPE. The experimental swelling limit for pure DOPE $\simeq$18 (Rand and Fuller, 1994). The phase diagram is further simplified by omitting coexistence regions and cubic phases. The phase diagram shows stable lamellar phases for DOPC rich systems, and at conditions of high hydration combined with low temperatures. At increased levels of DOPE and at elevated temperature or reduced hydration levels, an inverted hexagonal phase is preferred. The striking exception is a stable lamellar phase observed for pure DOPE at low temperatures and intermediate hydration levels. A so-called reentrant hexagonal-lamellar-hexagonal phase transition sequence occurs upon dehydration at low temperature (Gawrisch et al., 1992; Rand and Fuller, 1994). For mixed systems, down to a PC/PE ratio of 1:3, the rhombohedral phase is observed. It occurs in between the hexagonal and lamellar phases, at low hydration and low temperature.

Simulations have been performed at state points covering almost the entire phase diagram. DOPC/DOPE mixtures with the compositions 1:0, 6:1, 3:1, 1:1, 1:3, and 0:1 were studied. These were investigated at hydration levels ranging from 4 to 16 waters/lipid and at temperatures between 273 K and 320 K. Note that here, and in the remainder of the article, the hydration level indicates the amount of real water. The corresponding amount of CG water in the simulation is four times less, as a CG water represents four real water molecules. The state points simulated are indicated in the phase diagram of Fig. 1. All simulations have been performed with the GROMACS software package (version 3.0; Lindahl et al., 2001). Fully anisotropic pressure coupling (to a reference pressure of 1 bar) was applied allowing the box shape to deviate from rectangular. Starting configurations were obtained by stacking preequilibrated bilayers of the required composition into multilamellar stacks. Typically four bilayers were stacked on top of each other, each bilayer containing 512 lipids. Systems consisting of two larger bilayers each containing 6400 lipids were also simulated. The results do not depend significantly on the size of the system. Lamellar-to-inverted hexagonal phase transitions either occurred spontaneously, or were triggered by changing the temperature, hydration level, or composition. The thermotropic phase transitions occurred at a fixed hydration level, analogous to the gravimetric measurements of Rand and Fuller (1994). The transitions triggered by dehydration of the sample mimic the humidity controlled experiments of Yang and Huang (Yang et al., 2003).

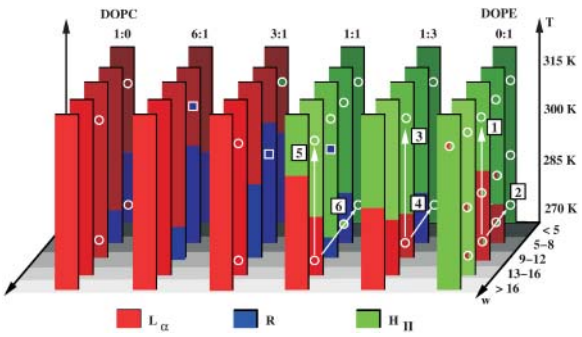

FIGURE 1 Schematic phase diagram for DOPC/DOPE, based on refs (Yang et al., 2003; Rand and Fuller, 1994). The approximate location of the lamellar (L_α), inverted hexagonal (H_{II}) and rhombohedral (R) phases are shown as a function of composition, temperature and hydration level w (water/lipids). The circles indicate the state points of the systems simulated. The fill color of the circles corresponds to the phase behavior predicted by the simulation. Circles filled by two colors indicate conditions for which the simulated lamellar phase is found to be metastable. Squares point to state conditions for which a stable rhombohedral phase has been simulated. The numbered arrows indicate some of the simulated phase transitions used for reference in the text.

To assess the conditions for which a stable rhombohedral phase might be observed an additional set of simulations was performed on small systems containing two bilayers of 64 lipids connected by a stalk. The starting configurations for these simulations were obtained from the simulations where stalks formed spontaneously. The state conditions for which the isolated stalk remains stable were determined by performing a large series of simulations in which the state conditions were systematically varied. The few systems with stable stalks were subsequently replicated to form larger bilamellar systems (512 lipids) and simulated on a microsecond time scale during which rearrangement of the stalks into a rhombohedral phase was observed. The set of simulations on small systems containing a stalk also served to assess the true thermodynamic stability of the lamellar phase with respect to the inverted hexagonal phase at a specific state point. Due to the energy barrier associated with stalk formation, the multilamellar phase can appear metastable on the time scale of the simulations (several microseconds). Starting from an intermediate structure along the lamellar-to-inverted hexagonal phase transition (i.e., a stalk), the pathway can be reversed upon changing the state conditions back to those of the target phase. Reappearance of the target phase at the end of the reversed pathway proves that the target phase is thermodynamically stable. Disappearance of the stalk shows the lamellar phase to be preferred, whereas elongation of the stalk indicates stability of the inverted hexagonal phase. Systems for which no spontaneous phase transition was observed, i.e., which remained lamellar, whereas preformed stalks clearly elongated are therefore considered metastable. The corresponding state conditions are indicated by a dual colored circle in Fig. 1. Another way of predicting the thermodynamic phase stability is by simulation of the spontaneous aggregation of the lipids from random solutions. Using this procedure, Shelley and coworkers were able to form an inverted hexagonal phase for a small system consisting of a coarse grained lipid/alkane mixture (Shelley et al., 2001). Also for the model considered in this work a random mixture of DOPE was shown to spontaneously form an inverted hexagonal phase (Marrink et al., 2004). This method, however, only appears to work fine for small systems and relative high hydration. Larger systems or systems at lower hydration levels easily get trapped into various kinds of metastable intermediate states, making the method less practical for predicting relative phase stability.

RESULTS AND DISCUSSION

L_α to H_{II} transition for pure DOPE

A thermotropic phase transition from a lamellar phase to an inverted hexagonal phase is illustrated in Fig. 2 for a

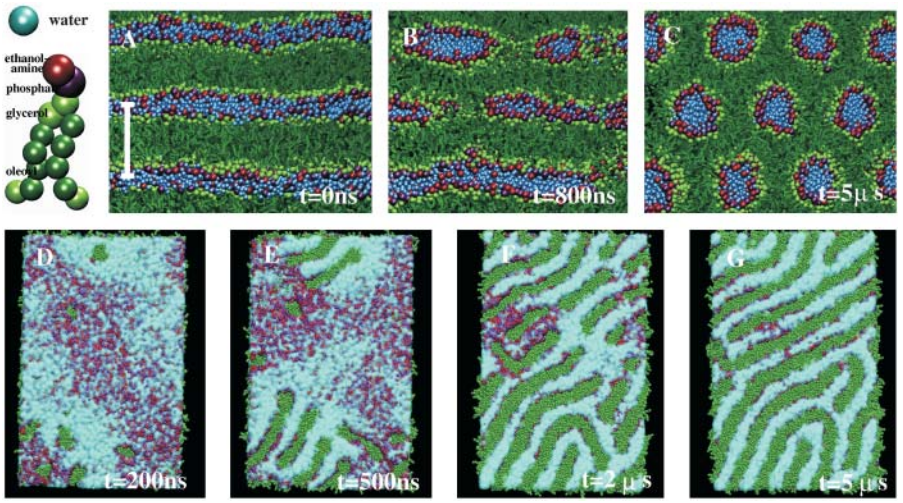

FIGURE 2 Thermotropic phase transition from a multilamellar to an inverted hexagonal phase for DOPE at low hydration (9 waters/lipid). (*A–C*) Close-ups of cross sections perpendicular to a system of four independent bilayers of 512 lipids each. The multilamellar stack of pure DOPE bilayers (*A*) is stable at $T = 273$ K. Upon increasing the temperature to $T = 308$ K, stalks form (*B*), which rearrange into a hexagonal lattice forming an inverted hexagonal phase (*C*). (*D–G*) View of a bilamellar system containing 6400 lipids on top, cutting through the stalks and water channels. Stalks are seen to form in the vicinity of each other (*D*). The stalks then elongate in a cooperative manner (*E*) leading to the formation of water channels (*F*). On length scales exceeding ~25 nm, cooperativity is lost and defects remain (*G*). The white bar in panel *A* indicates a length of 5 nm. The inset shows the coarse grained model for the DOPE lipid and the solvent, and indicates the color scheme used.

multilamellar DOPE system consisting of four bilayers of 512 lipids each at 9 waters/lipid (*transition 1* of Fig. 1). Initially (Fig. 2 *A*) the temperature of the system is 273 K and the multilamellar state is stable. Increasing the temperature to 308 K makes the system unstable. Connections between the lamellae (the so-called stalks) appear within hundreds of nanoseconds (Fig. 2 *B*). The stalks are not stable but elongate in a cooperative manner, forming the final inverted hexagonal phase within a few microseconds (Fig. 2 *C*). The inverted hexagonal phase consists of hexagonally packed water channels surrounded by lipid. The same phase transition can also be triggered by reducing the hydration level to 4 waters/lipid while keeping the temperature constant at 273 K (*transition 2* of Fig. 1).

The rate of stalk formation depends on the hydration level and the temperature of the system. Fig. 3 shows the rate of stalk formation as a function of the hydration level at two different temperatures. As the hydration level increases, the rate of stalk formation decreases from tens of nanoseconds (4 waters/lipid) to multi-μs (9 waters/lipid), all at 308 K. Lowering the temperature by 20 K decreases the rate of stalk formation by a factor of ~4. The frequency of stalk formation also depends on the membrane area considered and the presence of neighboring stalks. Stalk formation is positively correlated with the presence of another stalk within a distance $\simeq$10 nm, either between the same or between adjacent lamellae. At larger distances stalks form independently. The rates given above were obtained by visual inspection of the trajectories of systems consisting of four bilayers of 512 lipids each. The time between the beginning of the simulation and the time where a stalk first appeared was taken as the rate of stalk formation. The ranges provided indicate the spread in values obtained from multiple (typically 3) independent simulations.

Fig. 2, *D–G*, illustrates the stages of the phase transition process that occur after the initial stalk has formed in more detail. A simulation of a larger bilamellar system containing 6400 lipids and measuring 50 × 50 nm (lateral dimensions) shows that multiple stalks form in the vicinity of each other (Fig. 2 *D*). Initially the stalks exhibit radial symmetry, but spontaneous symmetry breaking occurs, leading to the elongation of the stalks (Fig. 2 *E*). Due to packing constraints the stalks can only grow linearly. The elongation rate of the stalks ranges from 0.05 to 0.2 nm ns^{-1}, with no clear correlation to either temperature or hydration level. These rates were obtained by averaging over all stalks formed during the time they could grow unrestrained, i.e., before running into other stalks or into their periodic image. Stalk elongation is a cooperative process, with neighboring stalks growing in the same direction (Fig. 2 *F*). At large distances this cooperativity is lost, however. Defects remain in the

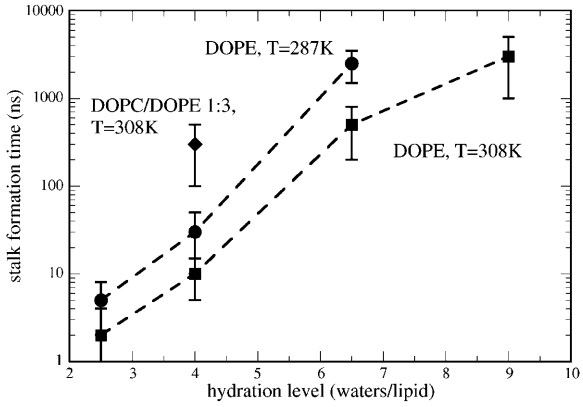

FIGURE 3 Rate of stalk formation as a function of the hydration level. All data were obtained from simulations of stacks of four bilayers, 512 lipids each. The times reported are the times required for the first stalk to appear. Circles denote pure DOPE systems at $T = 287$ K, squares pure DOPE at $T = 308$ K, and the diamond refers to a 1:3 DOPC/DOPE mixture also at 308 K. The error bars indicate the range in stalk formation times observed from multiple simulations.

hexagonal lattice due to the loss of cooperativity on this length scale (Fig. 2 *G*). Although the system gradually resolves such defects during a continuing simulation, a complete resolution of these defects is not observed on a microsecond timescale. For macroscopic systems the time required to complete such a phase transition is therefore expected to be milliseconds or longer.

The mechanism of transition from the initial formation of a stalk to the formation of the hexagonal phase has been the topic of an ongoing debate in the literature (e.g., Hui et al., 1983; Caffrey, 1985; Siegel et al., 1994, 1999; Cherezov et al., 2003; Rappolt et al., 2003). Our simulations show that correlated stalk elongation can drive the system directly into the hexagonal phase. Close to the actual transition temperature, based on theoretical calculations Siegel (1999) argues that stalk elongation is not the most energetically favorable transition pathway. Rather, the stalks rearrange into a hexagonally ordered phase similar to the rhombohedral phase, after which fusion between stalks leads to the formation of the inverted hexagonal phase. The lamellar-to-inverted hexagonal transitions observed in our simulations always proceed through stalk elongation. This suggests that a pathway with a rhombohedral like intermediate could be favorable at conditions very close to the phase boundary only.

No spontaneous stalk formation was observed at hydration levels of more than 12 waters/lipid or at reduced temperatures combined with hydration levels of more than 8 waters/lipid. Simulations of small systems with a preformed stalk reveal that the hexagonal phase is still formed in these cases. This observation indicates that the pure DOPE lamellar phase is a metastable phase, kinetically trapped on the timescale of the simulations (10 μs). A large hydration layer and/or low temperature prevents the rapid formation of stalks, as is apparent from extrapolation of the results shown in Fig. 3. The small region for which the lamellar phase of DOPE is found to be thermodynamically stable experimentally (see Fig. 1) is not reproduced by the simulations.

Structure of the DOPE H_{II} phase

In Fig. 4 the structure of the inverted hexagonal phase for pure DOPE is shown in more detail (Fig. 4 *A*). The ends of the lipid tails are arranged into hexagons, which define the unit cell of the lattice (Fig. 4, *B* and *C*). The lipid tails are able to pack into the hexagon without creating voids through a gradual tilting of their tails. This observation underlines the theoretical predictions made by Hamm and Kozlov (1998). The hexagonal spacing d_{hex}, related to the unit cell size $s = \frac{2}{\sqrt{3}} d_{hex}$, appears to be both temperature- and hydration level-dependent. In agreement with the experimental x-ray diffraction results (Rand and Fuller, 1994), the hydration level has the largest effect. For instance, at $T = 308$ K as the hydration level in the system is increased from 4 to 9 to 16 waters/lipid, there is an almost 50% increase of the hexagonal spacing from $d_{hex} = 4.5$ nm to 5.8 nm to 6.7 nm. Reducing the temperature from 308 K to 287 K at a fixed hydration level of 16 waters/lipid results in an increase of $<10\%$ (from 6.7 nm to 7.2 nm). The hexagonal spacings are in good quantitative agreement with the experimental observations. The absolute spacings predicted by the simulations are $\sim 10\%$ larger than those obtained experimentally; however, this is mainly an effect of coarse graining four methylene groups into one interaction site within the model used. The oleoyl tails of DOPE, containing 18 carbon groups, would ideally be modeled with 4.5 sites. As this is not possible they are modeled with five sites. The effective tail length is thus increased by $\sim 10\%$, increasing the hexagonal spacing by a similar amount.

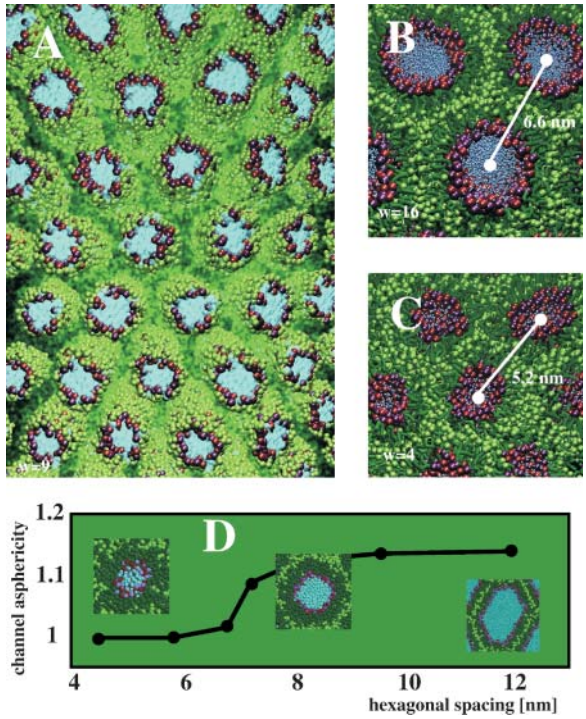

FIGURE 4 Structure of the hexagonal phase for pure DOPE systems at $T = 308$ K. The color scheme corresponds to Fig. 2. Panel *A* shows a system containing 6400 lipids at a hydration level $w = 9$ waters/lipid. Both the solvent and the lipid tails are semitransparent. Panels *B* and *C* show close-ups of the hexagonal unit cell at different levels of hydration (16 waters/lipid and 4 waters/lipid). The terminal lipid tail groups are colored a lighter shade of green to emphasize the hexagonal shape of the unit cell. The increasing hexagonal shape of water channels with increasing unit cell size is shown in panel *D*.

Regarding the shape of the water channels, a crossover from a spherical to a hexagonal shape has been observed experimentally (Turner and Gruner, 1992). In the experiment, it occurs at a unit cell size of ~ 7.5 nm (corresponding hexagonal spacing 6.5 nm). This is reproduced by the simulations. In Fig. 4 *D* we show the asphericity of the water channel geometry as a function of the hexagonal spacing. The asphericity is defined as the ratio between the largest and smallest radii of the channel. An asphericity of 1 describes

a circular geometry, a geometry of $\frac{2}{\sqrt{3}} = 1.15$ a perfect hexagon. Indeed our simulations show a circular shape for spacings below ~7 nm, whereas for larger spacings the water channel geometry tends to be hexagonal. In agreement with recent theoretical calculations (Malinin and Lentz, 2004), the shape of the water channels at hexagonal spacings corresponding to all but the lowest hydration levels below the experimental swelling limit (d_{hex} ~ 5–8 nm) is best characterized as intermediate in between spherical and hexagonal. At hydration levels beyond the experimental swelling limit the hexagonal unit cell becomes distorted (*rightmost picture* in Fig. 4 *D* was obtained at 40 waters/lipid). Experimentally excess water separates into a bulk water phase. In the relatively small simulation cells the water remains trapped inside the hexagonal phase leading to an apparent distortion of the lattice. In principle phase separation may occur inside the simulation cell. For small systems the energetic cost of sustaining the interface between the hexagonal and pure water phase is prohibitively high, however. Interestingly, at hydration levels exceeding 20 waters/lipid, preformed stalks spontaneously disappear.

L_α to H_{II} transition for mixed DOPC/DOPE

In comparison to DOPE, DOPC prefers lamellar phases. The bulky choline group of DOPC does not readily pack into an inverted phase. The experimentally determined phase diagram (Yang et al., 2003) of DOPC/DOPE mixtures at $T =$ 308 K shows that mixtures up to 1:1 still readily form inverted hexagonal phases (see Fig. 1). Decreasing the temperature or increasing the hydration level shifts this ratio toward a larger fraction of DOPE. The simulations reproduce the experimental phase behavior remarkably well. Both for systems consisting of a 1:3 and a 1:1 ratio of DOPC/DOPE the hexagonal phase can be formed upon dehydration (e.g., *transitions 4* and *6* in Fig. 1) or by an increase in temperature (*transitions 3* and *5*). The lamellar phase was found to be thermodynamically stable at higher hydration levels combined with a low temperature (273 K). At higher levels of DOPC the hexagonal phase was only observed in simulations at very low water content (4 waters/lipid). The phase transition pathway for the mixtures is the same as depicted in Fig. 2 for the pure DOPE system. The dynamics of the transition are slower with increasing amounts of DOPC, however. For instance, the rate of stalk formation drops by roughly an order of magnitude when comparing pure DOPE to a 1:3 DOPC/DOPE mixture (see Fig. 3). Stalk elongation still occurs at a similar rate as observed for the pure DOPE systems. Experimental evidence exists (Yang et al., 2003) for a nonhomogeneous mixing of the two components close to the phase border between the inverted hexagonal and the rhombohedral phase. This is inferred from the appearance of a distorted hexagonal lattice. In our simulations of mixed systems we did not observe a distorted hexagonal phase. The hexagonal lattices all have unit vector angles within 2° of the perfect hexagonal angle of 60°. Analysis of the distribution of DOPC and DOPE in the inverted hexagonal phase reveals homogeneous mixing of the two components. No evidence for lateral clustering in PC/PE systems has also recently been reported from atomistic simulations of lipid bilayers (De Vries et al., 2004), indicating that the choline and ethanolamine groups apparently mix well. In the inverted hexagonal phase an additional degree of freedom exists for the packing of the tails, however. Fig. 5 shows contour lines at relative high density for the PC and PE headgroups and for the terminal group of the lipid tails. The maximum of the distribution of the lipid headgroups is restricted to a circular region around the water channel, with no difference between the PC and PE headgroups. The lipid tail-ends have a maximum density at the interstitial region which is located furthest away from the channels. The mixing of the tails is not completely ideal. The terminal tail groups of DOPC

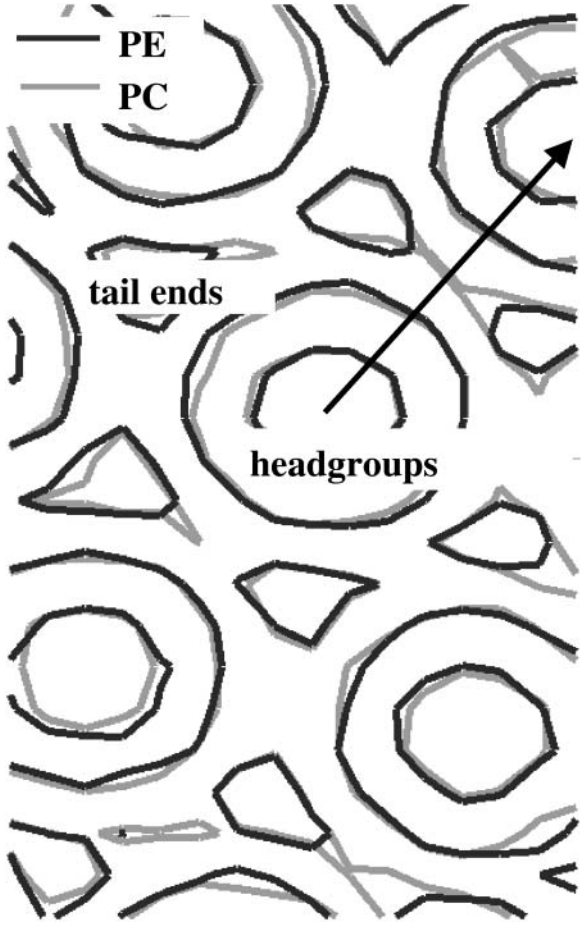

FIGURE 5 Isodensity contour lines for an inverted hexagonal phase of a DOPC/DOPE 1:1 mixture at $T = 308$ K and 10 waters/lipid. Regions of relative high density are shown for the PC/PE headgroups (*circular regions*), and for the terminal group of the oleoyl tails (*triangular regions*). The density profiles were obtained from averaging along the direction of the water channels during a microsecond simulation. The arrow represents one of the unit cell vectors.

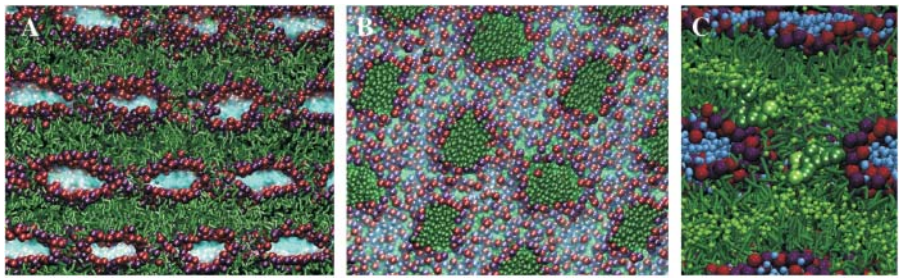

FIGURE 6 Stable rhombohedral phase for DOPC/DOPE mixture 6:1 at $T = 308$ K and a hydration level of 10 waters/lipid. Panel *A* shows a cross section cutting through the stalks and the lamellae, panel *B* a cut through the water layer revealing the hexagonal lateral packing of the stalks. Panel *C* shows a close-up of a stalk, with two individual lipids highlighted. Color scheme as in Fig. 2. The solvent in panels *A* and *B* is semitransparent.

exhibit an increased density at the positions along the unit cell vectors compared to DOPE. Since the volume available for the tails is smaller in the direction along the unit vector, the preference of the lipid with the smaller tail-to-headgroup volume, DOPC, can be rationalized.

Structure of the rhombohedral phase

In a narrow composition/temperature/hydration range Yang et al. (2003) recently reported the observation of a stable rhombohedral phase in DOPC/DOPE mixtures. By systematically studying the stability of stalks in small test systems we were also able to find conditions under which the rhombohedral phase appeared stable in the simulations. Fig. 6 shows images of the rhombohedral phase of a DOPC/DOPE 6:1 mixture, at a hydration level of 10 waters/lipid and $T = 308$ K. Stalks connecting the lamellae appear stable (Fig. 6 *A*). Instead of elongating, they remain spherical and rearrange laterally into a (distorted) hexagonal pattern (Fig. 6 *B*). The phase is stable on the time scale of the simulation (μs). Stable rhombohedral phases are also found for DOPC/DOPE 3:1 mixtures at $T = 298$ K and at 10 waters/lipid, and for the 1:1 composition at $T = 298$ K and 14 waters/lipid. These conditions are comparable to those determined experimentally (see the phase diagram in Fig. 1). The structure of a typical stalk is shown in Fig. 6 *C*. The stalk is composed entirely of the two contacting monolayers. The outer monolayers appear somewhat dimpled at the position of the stalk. Together with a tilting of the lipid tails around the stalk edges, this prevents the formation of energetically highly unfavorable voids. The molecular picture obtained from the simulations is in line with recent theoretical predictions of a voidless stalk structure (Kozlovsky et al., 2002; May, 2002).

It is also similar to the stalk structure observed during simulation of the fusion of lipid vesicles (Marrink and Mark, 2003) and as an intermediate in the simulated transition from an inverted cubic to an inverted hexagonal phase (Marrink and Tieleman, 2002).

CONCLUSION

In summary, we have shown that the mechanism of the lamellar-to-inverted hexagonal phase transition proceeds through stalk formation and subsequently through stalk elongation. Both stalk formation and elongation are found to be cooperative processes. The probability of formation of a stalk is enhanced in the vicinity of other stalks, occurring on a nano- to microsecond timescale. The rate of stalk elongation ranges from 0.05 to 0.2 nm ns^{-1} and is strongly correlated over distances up to tens of nanometers. Within a narrow hydration/composition range the stalks do not elongate but appear stable instead, rearranging into the rhombohedral phase.

We thank M. Kozlov, D. P. Tieleman, and H. J. C. Berendsen for their careful reading of the manuscript.

This research was supported by the Royal Academy of Sciences of the Netherlands (KNAW).

REFERENCES

Caffrey, M. 1985. Kinetics and mechanism of the lamellar gel lamellar liquid-crystal and lamellar inverted hexagonal phase-transition in phosphatidylethanolamine—a real-time x-ray-diffraction study using synchrotron radiation. *Biochemistry*. 24:6349–6363.

Cherezov, V., D. P. Siegel, W. Shaw, S. W. Burgess, and M. Caffrey. 2003. The kinetics of nonlamellar phase formation in dope-me: relevance to biomembrane fusion. *J. Membr. Biol.* 195:165–182.

Chernomordik, L. V., G. B. Melikyan, and Y. A. Chizmadzhev. 1987. Biomembrane fusion—a new concept derived from model studies using two interacting planar lipid bilayers. *Biochim. Biophys. Acta*. 906:309–352.

De Vries, A. H., A. E. Mark, and S. J. Marrink. 2004. The binary mixing behavior of phospholipids in a bilayer: a molecular dynamics study. *J. Phys. Chem. B*. 108:2454–2463.

Gawrisch, K., V. A. Parsegian, D. A. Hajduk, M. W. Tate, S. Gruner, N. Fuller, and R. P. Rand. 1992. Energetics of a hexagonal-lamellar-hexagonal phase transition sequence in dioleoylphosphatidylethanolamine membranes. *Biochemistry*. 31:2856–2864.

Hamm, M., and M. M. Kozlov. 1998. Tilt model of inverted amphiphilic mesophases. *Eur. Phys. J. B*. 6:519–528.

Hui, S. W., T. P. Stewart, and L. T. Boni. 1983. The nature of lipidic particles and their roles in polymorphic transitions. *Chem. Phys. Lipids*. 33:113–116.

Kozlov, M. M., and V. S. Markin. 1983. Possible mechanism of membrane-fusion. *Biofizika*. 28:242–247.

Kozlovsky, Y., L. V. Chernomordik, and M. M. Kozlov. 2002. Lipid intermediates in membrane fusion: formation, structure, and decay of hemifusion diaphragm. *Biophys. J*. 83:2634–2651.

Lindahl, E., B. Hess, and D. van der Spoel. 2001. GROMACS 3.0: a package for molecular simulation and trajectory analysis. *J. Mol. Mod.* 7:306–317.

Malinin, V. S., and B. R. Lentz. 2004. On the analysis of elastic deformations in hexagonal phases. *Biophys. J.* 86:3324–3328.

Marrink, S. J., A. H. de Vries, and A. E. Mark. 2004. Coarse-grained model for semiquantitative lipid simulations. *J. Phys. Chem. B.* 108:750–760.

Marrink, S. J., and A. E. Mark. 2003. The mechanism of vesicle fusion as revealed by molecular dynamics simulations. *J. Am. Chem. Soc.* 125:11144–11145.

Marrink, S. J., and D. P. Tieleman. 2002. Molecular dynamics simulation of spontaneous membrane fusion during a cubic-hexagonal phase transition. *Biophys. J.* 83:2386–2392.

May, S. 2002. Structure and energy of fusion stalks: the role of membrane edges. *Biophys. J.* 83:2969–2980.

Rand, R. P., and N. L. Fuller. 1994. Structural dimensions and their changes in a reentrant hexagonal-lamellar transition of phospholipids. *Biophys. J.* 66:2127–2138.

Rappolt, M., A. Hickel, F. Bringezu, and K. Lohner. 2003. Mechanism of the lamellar/inverse hexagonal phase transition examined by high resolution x-ray diffraction. *Biophys. J.* 84:3111–3122.

Shelley, J. C., M. Shelley, R. Reeder, S. Bandyopadhyay, P. B. Moore, and M. L. Klein. 2001. Simulations of phospholipids using a coarse-grained model. *J. Phys. Chem. B.* 105:9785–9792.

Siegel, D. P. 1999. The modified stalk mechanism of lamellar/inverted phase transitions and its implications for membrane fusion. *Biophys. J.* 76:291–313.

Siegel, D. P., and R. M. Epand. 1997. The mechanism of lamellar-to-inverted hexagonal phase transitions in phosphatidylethanolamine: Implications for membrane fusion mechanisms. *Biophys. J.* 73:3089–3111.

Siegel, D. P., W. J. Green, and Y. Talmon. 1994. The mechanism of lamellar-to-inverted hexagonal phase-transitions — a study using temperature-jump cryoelectron microscopy. *Biophys. J.* 66:402–414.

Smit, B., P. A. J. Hilbers, K. Esselink, L. A. M. Rupert, N. M. van Os, and A. G. Schlijper. 1990. Computer simulations of a water/oil interface in the presence of micelles. *Nature.* 348:624–625.

Turner, D. C., and S. M. Gruner. 1992. X-ray-diffraction reconstruction of the inverted hexagonal (hii) phase in lipid water-systems. *Biochemistry.* 31:1340–1355.

Yang, L., L. Ding, and H. W. Huang. 2003. New phases of phospholipids and implications to the membrane fusion problem. *Biochemistry.* 42: 6631–6635.

Yang, L., and H. W. Huang. 2002. Observation of a membrane fusion intermediate structure. *Science.* 297:1877–1879.